Nuclear Medicine Communications, 2000, **21,** 269–276

Nuclear Medicine Communications

A non-invasive isotope dilution technique for quantifying hepatic blood flow using radiolabelled red blood cells

W.K. YU,[1]* P.K.H. CHOW,[2] S. SOMANESAN,[1] T.H. NG,[3] F.X. SUNDRAM,[1] S.T.F. CHAN,[4] K.C. SOO,[2] S.E. AW[1] and S.M. SHAW[5]

Departments of [1]Nuclear Medicine, [2]General Surgery and [3]Experimental Surgery, Singapore General Hospital, [4]Department of Surgery, National University of Singapore and [5]Department of Medicinal Chemistry, Purdue University, USA

Received 13 January 1999, in revised form 16 July 1999 and accepted 24 August 1999

Summary

Clinically significant changes in hepatic haemodynamics accompany the development of portal hypertension, hepatocellular carcinoma, liver metastases and liver cirrhoses, and after major liver resection. Hepatic blood flow parameters, such as hepatic arterial flow (HAF), hepatic portal flow (HPF), total hepatic blood flow (THBF) and hepatic perfusion index (HPI), are useful adjuncts to the diagnosis of liver pathology, the evaluation of disease progress and prognostication. Here, we describe a non-invasive method that combines the measurement of these parameters in a single study in real time.

Red blood cells from eight pigs were labelled with $^{99}Tc^{m}$ using an *in-vitro* method and re-injected into the pigs. Data acquisition over the heart, lungs, liver and kidneys was started immediately and a blood sample was obtained 15 min post-injection. Hepatic arterial flow was determined from the ratio of the maximum gradients between the integrated time–activity curve of the left ventricle and the first-pass time–activity curve of the liver before the peak of the kidneys time–activity curve. The hepatic perfusion index was determined by comparing the slope of the liver time–activity curve before and after the kidney peak. Hepatic portal flow was determined from the hepatic arterial flow and the hepatic perfusion index, and total hepatic blood flow was determined as the sum of arterial and portal flow. The results were compared against those obtained from a clearance method using $^{99}Tc^{m}$-DISIDA.

The average hepatic perfusion index was 0.38, and the average hepatic arterial flow and hepatic portal flow were 168.3 ± 52.9 and 274.6 ± 60.1 ml · min^{-1} respectively. The average total hepatic blood flow was 442.8 ± 53.5 ml · min^{-1}, while the total hepatic flow determined by $^{99}Tc^{m}$-DISIDA clearance was 419.7 ± 62.6 ml · min^{-1}. No significant difference in total hepatic blood flow was found between the two methods. The results of this study show that it is possible to obtain all hepatic haemodynamics data in a single study using a non-invasive method. (© 2000 Lippincott Williams & Wilkins)

Introduction

The development of liver disease, such as portal hypertension [1] and liver malignancies, is associated with changes in liver haemodynamics [2, 3]. Significant changes in hepatic blood flow also occur after major liver resection [4, 5] and are believed to be important for recovery of liver function and regeneration [6, 7]. In addition, the development of liver cirrhosis is accompanied by an increase in the hepatic perfusion index [8]. Portal-systemic shunting is also a feature of end-stage liver disease [9]. The measurement and monitoring of liver blood flow are thus useful adjuncts in the diagnosis, prognosis and management of these conditions.

A number of non-invasive methods to measure hepatic haemodynamics are currently available, including Doppler ultrasonography and various clearance techniques. Although Doppler ultrasonography is a convenient

*Address all correspondence to Sidney Yu, Department of Nuclear Medicine, Singapore General Hospital, Outram Road, Singapore 169608.

method, turbulence within vessels, non-linear flow [10], interference from gaseous intestinal contents and inter-operator variability [11] all conspire to make interpretation difficult. Clearance techniques using radiopharmaceuticals such as Indo-cyanine green and $^{99}Tc^{m}$-DISIDA are also convenient methods, but hepatic clearance depends on hepatocellular function and this varies with disease state in an unpredictable manner [12].

Using an indicator dilution technique, Peters *et al*. [13] described a general method to determine organ blood flow based on the fractionation of the cardiac output delivered to the organ. The liver, however, is an organ with a dual blood supply, whereas the technique developed by Peters *et al*. is based on the assumption of a single blood supply. Using the principles of Peters and co-workers' technique, Tindale *et al*. [14] reported a novel approach to the determination of total hepatic blood flow (THBF) by measuring hepatic arterial flow (HAF) and hepatic portal flow (HPF) separately.

O'Connor *et al*. [15] independently developed a method to measure the hepatic perfusion index (HPI) using $^{99}Tc^{m}$-DTPA, and Shikare *et al*. [8] also applied similar principles to measure this index in patients. The hepatic perfusion index is the ratio of HAF/THBF. It is possible, in theory, to determine hepatic portal flow based on the HPI and hepatic arterial flow. Total hepatic blood flow can then subsequently be determined. This paper describes a method that combines the determination of HAF, HPI, HPF and THBF in a single study. Tindale and co-workers' [14] method to determine THBF makes use of deconvolution analysis and is based on the plateau heights of the HAF and HPF portions of the liver time–activity curve. This study determines THBF based on HPI without using deconvolution analysis. Hence, the method described may be more convenient and the HPI generated could also be used to assess the condition of the liver as described by O'Connor *et al*. [15] and Shikare *et al*. [8].

Materials and methods

General procedures

Yorkshire pigs weighing 17–27 kg were anaesthetized using Ketamine and Thiopental according to a protocol previously established in our institution [16]. Catheters were then inserted into the left and right internal jugular veins of the animals using an open technique. Ten millilitres of blood were drawn and spun and the red blood cells were collected and labelled with $^{99}Tc^{m}$ using an *in-vitro* technique [17] with a labelling efficiency greater than 90%. An aliquot (260–444 MBq) of the $^{99}Tc^{m}$-labelled red blood cells ($^{99}Tc^{m}$-RBC) in a volume less than 1 ml was injected as a bolus dose into the animal via the right internal jugular catheter; this was immediately flushed with a 10 ml bolus dose of normal saline. Data acquisition for the heart and liver was started simultaneously with the $^{99}Tc^{m}$-RBC injection. We used a gamma camera (GE Starcam) equipped with a low-energy, all-purpose, parallel-hole collimator. Acquisition was done in a 128×128 format at 1 s per frame for the first 60 s and then at 1 min per frame for the next 14 min. Regions of interest were drawn over the heart, left ventricle, lungs, liver, kidney and the aorta. A 1 ml blood sample was drawn from the left internal jugular catheter 15 min after the $^{99}Tc^{m}$-RBC injection.

Correction for scatter and computation of time–activity curves

The net counts in the regions of interest (ROI) of the liver and left ventricle were determined by taking the raw counts and correcting for scatter according to the method described by Miki *et al*. [18]. The corrected liver counts were determined using equation (1) and the corrected left ventricle counts were determined using equation (2):

$$L_{\text{corrected}}(t) = L_{(t)} - \frac{\int_0^{t^0} L(t)\mathrm{d}t \text{ x } H(t)}{\int_0^{t^0} H(t)\mathrm{d}t} \qquad (1)$$

where $L_{\text{corrected}}(t)$ = corrected counts in liver ROI at time t, $L(t)$ = raw counts in liver ROI at time t, t^0 = time when liver uptake started and $H(t)$ = raw counts in heart ROI.

$$LV_{\text{corrected}}(t) = LV(t) - \frac{\text{number of pixels in left ventricle ROI} \times Lu(t)}{\text{number of pixels in lung ROI}} \qquad (2)$$

where $LV_{\text{corrected}}(t)$ = corrected counts in left ventricle ROI at time t, $LV(t)$ = raw counts in left ventricle ROI at time t and $Lu(t)$ = counts in lung ROI at time t.

The integrated time–activity curve of the left ventricle and the time–activity curve of the liver were plotted. The renal first-pass time–activity curve was plotted and the time to reach the peak was used to indicate the division of the arterial and portal components of the THBF [8].

Determination of the hepatic perfusion index

The hepatic perfusion index was determined using the methods described by Shikare *et al*. [8] and O'Connor *et al*. [15]. A linear fit was applied to the hepatic time–activity curve for 3 s before and after the kidney peak. The average slopes of the two fits before and after the kidney peak were used to calculate the HPI:

$$\text{HPI} = H1/(H1 + H2) \qquad (3)$$

where HPI = hepatic perfusion index, $H1$ = slope of the arterial portion and $H2$ = slope of the portal portion.

Determination of hepatic arterial flow

The HAF was determined by equation (3) developed by Peters *et al*. [13]:

$$\mathrm{HAF} = (g_k/g_a)(\alpha/\gamma)$$

where HAF = hepatic arterial flow, g_k = maximum gradient of the arterial component of the liver time–activity curve, g_a = maximum gradient of the integrated time–activity curve of the left ventricle, γ = a conversion factor that converts count rate of the left ventricle ROI to $\mathrm{MBq \cdot ml^{-1}}$ and α = a correction factor for detector sensitivity, organ depth and photon attenuation.

Peters *et al*. [13] determined that, if the dose is measured on the gamma camera surface, α is limited to the attenuation coefficient only, which Tindale *et al*. [14] established as $0.123 \cdot \mathrm{cm^{-1}}$. The depth of the liver can be determined by taking a lateral view of the liver and measuring the distance between the skin surface depicted by a radioactive marker and the centre of the liver [13, 14]. The conversion constant, γ, was determined by equation (4), as described by Tindale *et al*. [14]:

$$\gamma = HV/T \quad (4)$$

where H = count rate of left ventricle ROI 15 min post-injection, V = volume of blood sample counted and T = count rate of the blood sample.

Determination of hepatic portal flow and total hepatic blood flow

The HPF and THBF were calculated using equations (5) and (6) respectively:

$$\mathrm{HPF} = \mathrm{HAF}/\mathrm{HPI} \times (1 - \mathrm{HPI}) \quad (5)$$

$$\mathrm{THBF} = \mathrm{HAF} + \mathrm{HPF} \quad (6)$$

Validation of results by $^{99}Tc^m$-DISIDA hepatic clearance

The hepatic blood flow of the experimental pigs was also determined by $^{99}Tc^m$-DISIDA using the procedures described by Rypins *et al*. [19]. On a separate occasion, the pigs were injected with 37–111 MBq of $^{99}Tc^m$-DISIDA via the internal jugular catheters into the systemic circulation. One-millilitre blood samples were drawn from the contralateral jugular vein 0.5, 1, 2, 4, 6, 8 and 10 min post-injection and the blood samples were counted in a NaI scintillation counter. The dose injected was determined by weighing the syringe before and after the injection and comparing against a reference standard.

The data were plotted into a two-compartment model and the HBF calculated as follows:

$$\mathrm{HBF} = \frac{\text{dose injected}}{(x_1/s_1) + (x_2/s_2)} \quad (7)$$

where $x_1 = x$ intercept of the first compartment, s_1 = slope of the first compartment, $x_2 = x$ intercept of the second compartment and s_2 = slope of the second compartment.

Results

The HPI ranged from 0.21 to 0.53, with an average of 0.38 and a standard deviation of 0.11 (Table 1). A liver time–activity curve before and after the kidney peak is shown in Fig. 1. The average HAF determined was $168.3 \pm 52.9\ \mathrm{ml \cdot min^{-1}}$ and the average HPF was $274.6 \pm 60.1\ \mathrm{ml \cdot min^{-1}}$. The average THBF was $442.8 \pm 53.5\ \mathrm{ml \cdot min^{-1}}$ (Table 1). After correction for body weight, HAF was $7.9 \pm 2.8\ \mathrm{ml \cdot min^{-1} \cdot kg^{-1}}$, HPF was $12.6 \pm 2.0\ \mathrm{ml \cdot min^{-1} \cdot kg^{-1}}$ and THBF was $20.3 \pm 1.9\ \mathrm{ml \cdot min^{-1} \cdot kg^{-1}}$ (Table 2). An integrated time–activity curve of the left ventricle and a time–activity curve of the liver are shown in Fig. 1.

The average THBF determined by $^{99}Tc^m$-DISIDA clearance was $419.7 \pm 62.6\ \mathrm{ml \cdot min^{-1}}$. After correction for body weight, THBF was $19.4 \pm 2.4\ \mathrm{ml \cdot min^{-1} \cdot kg^{-1}}$ (Table 3). A two-compartment clearance curve of $^{99}Tc^m$-DISIDA is shown in Fig. 2. The THBF determined by the $^{99}Tc^m$-RBC dilution method and that by the $^{99}Tc^m$-DISIDA clearance method were shown to be similar (Table 4) using Student's *t*-test ($P > 0.05$).

Table 1. Hepatic perfusion index (HPI), hepatic arterial flow (HAF), hepatic portal flow (HPF) and total hepatic blood flow (THBF) of pigs determined using $^{99}Tc^m$-RBC.

	Pig								*Mean*
	1	*2*	*3*	*4*	*5*	*6*	*7*	*8*	*±s*
Body weight (kg)	22.1	25.4	27.3	17.5	16.9	22.6	20.6	22.1	21.8 ± 3.5
HPI	0.30	0.39	0.31	0.32	0.46	0.51	0.53	0.21	0.38 ± 0.11
HAF ($\mathrm{ml \cdot min^{-1}}$)	142.8	190.6	160.3	113.8	181.7	214.5	252.2	90.4	168.3 ± 52.9
HPF ($\mathrm{ml \cdot min^{-1}}$)	330.9	292.1	353.3	239.5	210.4	209.6	225.7	334.9	274.6 ± 60.1
THBF ($\mathrm{ml \cdot min^{-1}}$)	473.7	482.7	513.6	353.3	392.1	424.1	477.9	425.3	442.8 ± 53.5

Table 2. Hepatic arterial flow (HAF), hepatic portal flow (HPF) and total hepatic blood flow (THBF) of pigs after correction for body weight.

	Pig								*Mean*
	1	*2*	*3*	*4*	*5*	*6*	*7*	*8*	*±s*
Body weight (kg)	22.1	25.4	27.3	17.5	16.9	22.6	20.6	22.1	21.8±3.5
HAF ($ml \cdot min^{-1} \cdot kg^{-1}$)	6.5	7.5	5.9	6.5	10.8	9.5	12.2	4.1	7.9±2.8
HPF ($ml \cdot min^{-1} \cdot kg^{-1}$)	15.0	11.5	12.9	13.7	12.5	9.3	11.0	15.1	12.6±2.0
THBF ($ml \cdot min^{-1} \cdot kg^{-1}$)	21.4	19.0	18.8	20.2	23.2	18.8	23.2	19.2	20.3±1.9

Table 3. Hepatic blood flow of the pigs determined by $^{99}Tc^{m}$-DISIDA clearance method.

	Pig								*Mean*
	1	*2*	*3*	*4*	*5*	*6*	*7*	*8*	*±s*
Body weight (kg)	22.1	25.4	27.3	17.5	16.9	22.6	20.6	22.1	21.8±3.5
HBF ($ml \cdot min^{-1}$)	418.4	436.7	536.2	317.7	408.6	372.4	419.1	448.5	419.7±62.6
HBF ($ml \cdot min^{-1} \cdot kg^{-1}$)	18.9	17.2	19.6	18.2	24.2	16.5	20.3	20.3	19.4±2.4

Table 4. Comparison of hepatic blood flow determined by $^{99}Tc^{m}$-RBC and $^{99}Tc^{m}$-DISIDA.

	Pig								*Mean*
	1	*2*	*3*	*4*	*5*	*6*	*7*	*8*	*±s*
HBF ($ml \cdot min^{-1}$)									
$^{99}Tc^{m}$-RBC	473.7	482.7	513.6	353.3	392.1	424.1	477.9	425.3	442.8±53.5
$^{99}Tc^{m}$-DISIDA	418.4	436.7	536.2	317.7	408.6	372.4	419.1	448.5	419.7±62.6
HBF ($ml \cdot min^{-1} \cdot kg^{-1}$)									
$^{99}Tc^{m}$-RBC	21.4	19.0	18.8	20.2	23.2	18.8	23.2	19.2	20.3±1.9
$^{99}Tc^{m}$-DISIDA	18.9	17.2	19.6	18.2	24.2	16.5	20.3	20.3	19.4±2.4

Discussion

The development of many liver diseases is associated with changes in the haemodynamics of liver blood flow. Major hepatectomy also gives rise to significant changes to liver blood flow, which is believed to be related to recovery and regeneration of the liver. The measurement of liver haemodynamics would be a useful adjunct to the diagnosis of liver pathology, the evaluation of disease progress and prognostication.

Existing methods for quantifying absolute hepatic blood flow (other than Doppler ultrasonography) may be classified as either clearance techniques or indicator dilution techniques [20]. Clearance techniques use agents that are highly extracted into the liver (e.g. indocyanine green, propanolol, lidocaine) and are based on the premise that, when liver extraction is high, hepatic clearance approximates hepatic blood flow. The liver extraction efficiencies of these agents are, however, decreased in various disease states in an inconsistent manner.

Indicator dilution techniques makes use of Fick's principle. The method is invasive and therefore not used routinely in clinical practice. Labelled agents such as red blood cells and human serum albumin are injected directly into the portal vein or hepatic artery (inflow) and blood is sampled serially from the hepatic vein (outflow). A variant of this technique is indicator fractionation, which uses radioactive inert gases such as ^{133}Xe and ^{85}Kr or radiolabelled microspheres. Sacrifice of the experimental animal is required and this technique has limited application in clinical practice.

Doppler ultrasonography is the most practical non-invasive method used to measure hepatic blood flow in clinical practice. Portal and hepatic arterial blood flow are measured separately and then summed [21]. Although convenient and non-invasive, its accuracy is highly operator-dependent [11] and it is subjected to significant

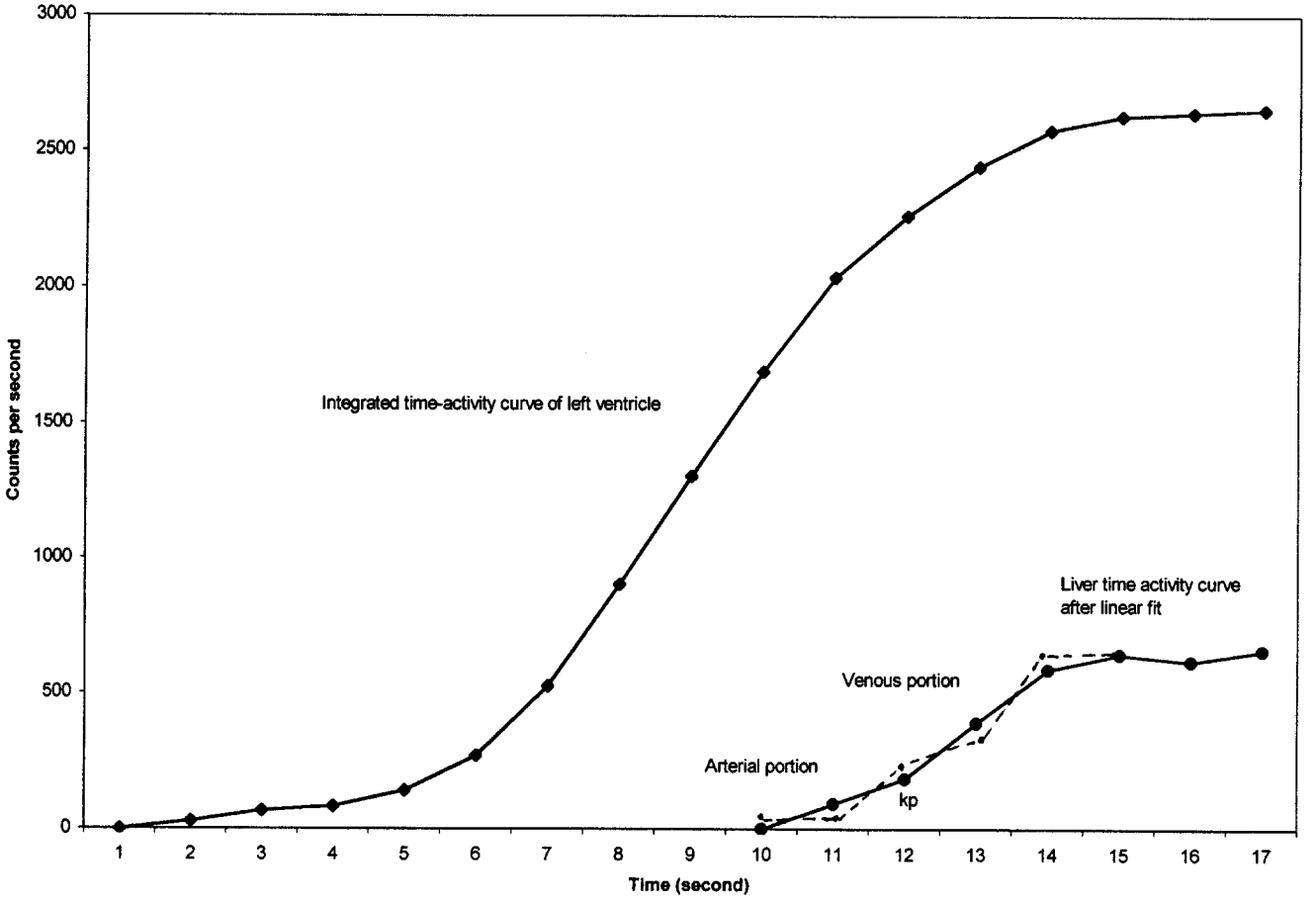

Fig. 1. Integrated time–activity curve of the left ventricle and liver time–activity curve after linear fit. The dotted line is the real liver time–activity curve before linear fit.

interference from the presence of abdominal gas [21]. The presence of aberrant vasculature (a common occurrence) must be accounted for and poses a serious problem.

This study was carried out to quantify total hepatic blood flow using $^{99}Tc^{m}$-RBC in a non-invasive way based on the dilution approach. Peters *et al*. [13] described a general method for this technique. The advantages of Peters and co-workers' technique include its non-invasive nature and the avoidance of complicated mathematical analysis, such as deconvolution analysis, which is used in many hepatic blood flow studies. Peters and co-workers' technique, however, describes the determination of blood flow in an organ with a single blood supply. Although Peters *et al*. [13] described the method as being independent of bolus width provided that it is not excessively prolonged or fragmented, it remained unclear if this technique can be applied to an organ with a dual blood supply. Nevertheless, Peters and co-workers' technique should be useful in measuring the arterial input of the total hepatic blood flow.

Based on the technique of Peters *et al*. [13], Tindale *et al*. [14] calculated hepatic blood flow by measuring hepatic arterial flow and hepatic portal flow separately, and showed that it is possible to determine total hepatic blood flow following Tindale's approach and using Peters' technique. One could, however, avoid the relatively complicated deconvolution analysis used by Tindale *et al*. by making use of the hepatic perfusion index as described in this study. Determination of this index using a linear fit of the liver time–activity curve has been reported by both O'Connor *et al*. [15] and Shikare *et al*. [8].

Changes to the hepatic perfusion index are reported to be a very sensitive index of the development of liver malignancies and a potentially useful diagnostic tool [22–24]. One advantage of our method is that the clinical usefulness of the index could be expanded, since this approach enables the index to be translated into actual flow. Another advantage of this method is that one could obtain all the hepatic haemodynamic parameters

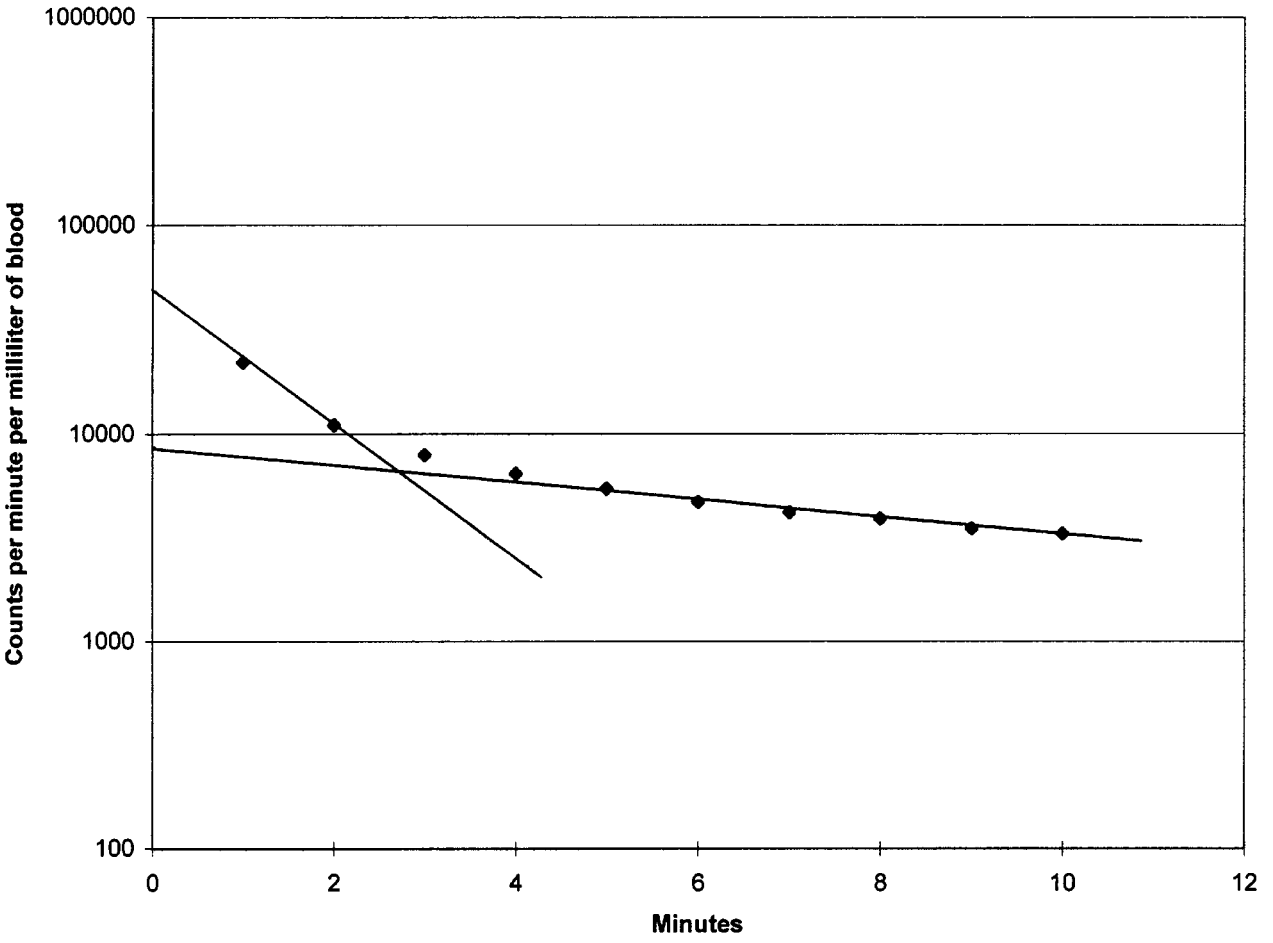

Fig. 2. $^{99}Tc^{m}$-DISIDA clearance curve.

as well as the cardiac output in a single study in real time.

We chose $^{99}Tc^{m}$-RBC over other non-diffusible intravascular tracers in this study because $^{99}Tc^{m}$-RBC does not leak out of the bloodstream as fast as $^{99}Tc^{m}$-albumin and, unlike $^{99}Tc^{m}$-DTPA, is not excreted by the kidney, thereby allowing it enough time to achieve complete and uniform distribution. One disadvantage of using $^{99}Tc^{m}$-RBC is a more complicated preparation procedure.

The results of this study agree well with published physiological data. A healthy 70-kg man is generally assumed to have a hepatic blood flow of about 1350 $ml \cdot min^{-1}$ [25]. This corresponds to a hepatic blood flow of 19.2 $ml \cdot min^{-1} \cdot kg^{-1}$ and is similar to the values obtained for total hepatic blood flow in this study using $^{99}Tc^{m}$-RBC (20.3 $ml \cdot min^{-1} \cdot kg^{-1}$). These results are also similar to and correlate well with values of total hepatic blood flow obtained by $^{99}Tc^{m}$-DISIDA clearance (19.4 $ml \cdot min^{-1} \cdot kg^{-1}$). The hepatic perfusion index of 0.38 in this study concurs with a value of 0.356 in healthy man [8], although Shilkare *et al*. also showed that the index is increased in patients with cirrhosis and also in non-cirrhotic portal hypertension.

The results of this study also agree well with most of the hepatic blood flow values published by other research groups using various methods. Ohnhaus *et al*. [26] measured total hepatic blood flow in man using ^{133}Xe. The liver blood flow determined was 1356 ± 382 $ml \cdot min^{-1}$, which would be 19.4 ± 5.4 $ml \cdot min^{-1} \cdot kg^{-1}$ body weight assuming a body weight of 70 kg. Total hepatic blood flow, as measured by Ha-Kawa and Tanaka [27] using $^{99}Tc^{m}$-GSA, was 1603 ± 144 $ml \cdot min^{-1}$, which would be 22.9 ± 2.0 $ml \cdot min^{-1} \cdot kg^{-1}$ body weight. The hepatic blood flow in normal humans measured by Munoz *et al*. [25] using indocyanin green and $^{99}Tc^{m}$-DISIDA was 1224 and 1384 $ml \cdot min^{-1}$ respectively, corresponding to 17.5 $ml \cdot min^{-1} \cdot kg^{-1}$ by indocyanine green and 19.8 $ml \cdot min^{-1} \cdot kg^{-1}$ by $^{99}Tc^{m}$-DISIDA. Total hepatic

blood flow measured by Cohn *et al*. [28] using indocyanine green and ^{131}I-human serum albumin in healthy subjects was 1380 and 1352 $ml \cdot min^{-1}$ respectively. This translates to a hepatic blood flow of 19.7 and 19.3 $ml \cdot min^{-1} \cdot kg^{-1}$ by indocyanine green and ^{131}I-human serum albumin respectively. On the other hand, our results differ from those of Mathie [29] using ^{85}Kr in dogs (100–130 $ml \cdot min^{-1} \cdot 100\ g^{-1}$ liver weight) and those of Miki *et al*. [18] in man (900 $ml \cdot min^{-1}$).

The use of $^{99}Tc^{m}$-DISIDA clearance as a comparison in this study may not be adequate. $^{99}Tc^{m}$-DISIDA clearance only shows the THBF and it does not provide any data on HAF, HPF and HPI. One problem of using $^{99}Tc^{m}$-RBC over $^{99}Tc^{m}$-DTPA is the visualization of the spleen in some pigs, due to the damage sustained by RBC during the labelling process. Scatter from spleen into the liver and left ventricle ROI may be significant, but was not addressed in our studies. The basic assumption of the technique of Peters *et al*. [13] is that the maximum gradient of the organ time–activity curve occurs before the minimum transit time through the organ, and this appears to be true in organs like kidney or spleen; however, we have no data to show that the same assumption is met in liver. Another assumption in this study is that there is a long enough temporal separation between tracer arrival via hepatic artery and portal vein as described by Tindale *et al*. [14]. Since we only analysed the first 20 s (a first-pass cycle of RBC is approximately 20 s in this study) and we assumed that $^{99}Tc^{m}$-RBC remained in the liver before minimum transit occurred, we did not correct for re-circulation.

Another potential error in this study was the assigning of the left ventricle ROI. The left anterior oblique view as employed in human heart scans does not give a good separation of the left ventricle. In the pig, anterior views produce better images, in which the left ventricle is minimally separated but the assignment of the left ventricle may still be susceptible to error.

There are other more serious potential errors in this study. The hepatic perfusion index is determined by taking the gradients of the portions of the liver curves 3 s before and after the kidney peak. However, the first-pass liver time–activity curve is not always linear before and after the kidney peak. The regression coefficients observed in this study ranged from 0.9955 to 0.8143. Also, there is not enough data points from each side of the curve to produce a result with minimal statistical error. In addition, the radioactivity of the arterial phase is leaving the liver during the portal phase, decreasing the gradient of the portal phase. Consequently, the hepatic perfusion index is increased. This is more prominent in our human trials. Finally, as the arterial input is faster than the portal input, the ratio of the gradients may not be equal to the ratio of blood flows. Additional correction factors may be required. Our results are based on a small sample size; further validation is therefore necessary.

Acknowledgements

The authors acknowledge a Singapore General Hospital Research Grant for the funding of this study. They are also grateful to Dr Peter Mack and his staff at the Department of Experimental Surgery, Singapore General Hospital, and Dr Terence Chua of the National Heart Centre, Singapore, for their enthusiastic support of this project.

References

1. Sherlock S, Dooley J. The portal system and portal hypertension. In: Sherlock S, Dooley J, eds. Diseases of the liver and biliary system, 10 edn. Oxford: Blackwell, 1998: 135–180.
2. Jakab F, Rath Z, Schmal F, Nagy P, Faller J. Changes in hepatic haemodynamics due to primary liver tumours. *HPB Surg* 1996; **9:** 245–248.
3. Cooke DA, Parkin A, Wiggins P *et al*. Hepatic perfusion index and the evolution of liver metastases. *Nucl Med Commun* 1987; **8:** 970–974.
4. Hanna S, Pagliarello G, Ing A. Liver blood flow after major hepatic resection. *Can J Surg* 1988; **31:** 363–368.
5. Kanematsu T, Takenaka K, Furuta T *et al*. Acute portal hypertension associated with liver regeneration: Analysis of early postoperative death. *Arch Surg* 1985; **120:** 1303–1308.
6. Kawasaki T, Moriyasu F, Kimura T, Someda H, Fukuda Y, Ozawa K. Changes in portal flow consequent to partial hepatectomy: Doppler estimation. *Radiology* 1991; **180:** 373–375.
7. Rabinovici N, Weiner E. Hemodynamic changes in the hepatectomised liver of the rat and their relationship to regeneration. *J Surg Res* 1963; **3:** 3–7.
8. Shikare SV, Bashir K, Abraham P *et al*. Hepatic perfusion index in portal hypertension of cirrhotic and non-cirrhotic aetiologies. *Nucl Med Commun* 1996; **17:** 520–522.
9. Bosch JM, Navasa JC, Garcia-Pagan A *et al*. Portal hypertension. *Med Clin North Am* 1989; **73:** 931–953.
10. Daigle RJ, Starvos AT, Lee RM. Overestimation of velocity and frequency values by multielement linear array dopplers. *J Vasc Tech* 1990; **14:** 206–213.
11. Sabba C, Merkel C, Zoli M *et al*. Interobserver and interequipment variability of echo-doppler examination of the portal vein: Effect of a cooperative training program. *Hepatology* 1995; **21:** 428–433.
12. Groszman RJ. The measurement of liver blood flow using clearance technique. *Hepatology* 1983; **3:** 1039–1040.
13. Peters AM, Gunasekera RD, Henderson BL *et al*. Non-invasive measurement of blood flow and extraction fraction. *Nucl Med Commun* 1987; **8:** 823–837.
14. Tindale WB, Barber DC, Smart HL *et al*. Liver blood flow: Non-invasive estimation using a gamma camera. *Proc Inst Mech Eng [H]* 1992; **206:** 88–103.

15. O'Connor MK, Krom RF, Carton EG *et al*. Ratio of hepatic arterial to portal venous blood flow: Validation of radionuclide technique in an animal model. *J Nucl Med* 1992; **33:** 239–245.
16. Chow PKH, Jeyaraj P, Tan SY, Fook Cheong S, Soo KC. Serial ultrasound-guided percutaneous liver biopsy in a partial hepatectomy porcine model: A new technique in the study of liver regeneration. *J Surg Res* 1997; **70:** 134–137.
17. Danpure HJ, Osman S. Methods of radiolabelling blood cells. In: Sampson C, ed. Textbook of radiopharmacy: Theory and practice. New York: Gordon & Breach, 1990: 213–215.
18. Miki K, Kubota K, Kokudo N *et al*. Asialoglycoprotein receptor and hepatic blood flow using Technetium-99m-DTPA-galactosyl human serum albumin. *J Nucl Med* 1987; **38:** 1798–1807.
19. Rypins EB, Milne N, Sarfeth IJ *et al*. Quantitation and fractionation of nutrient hepatic blood flow in normal persons, in persons with portal hypertensive cirrhosis, and after small-diameter portacaval H grafts. *Surgery* 1998; **104:** 335–342.
20. Mathie RT, Wheatley AM, Blumgart LH. Liver blood flow: Physiology, measurement and clinical relevance. In: Blumgart LH, ed. Surgery of the liver and biliary tract, 2nd edn. London: Churchill Livingstone, 1994: 95–110.
21. Bombelli L, Genitoni V, Biasi S, Materozzo C, Bonfanti G. Liver haemodynamic flow balance by image-directed doppler ultrasound evaluation in normal subjects. *J Clin Ultrasound* 1991; **19:** 257–262.
22. Leen E, Goldberg JA, Anderson JR, Robertson J, Cooke TG, McArdle CS. Hepatic perfusion changes in patients with liver metastases: Comparison with those patients with cirrhosis. *Gut* 1993; **34:** 554–557.
23. Leen E, Goldberg JA, Robertson J *et al*. Early detection of occult colorectal hepatic metastases using duplex colour doppler sonography. *Br J Surg* 1993; **80:** 1249–1251.
24. Leen E, Angerson WJ, Wotherspoon H, Moule B, Cooke TG, McArdle CS. Comparison of the doppler perfusion index and intraoperative ultrasonography in diagnosing colorectal liver metastases. *Ann Surg* 1994; **220:** 663–667.
25. Munoz C, Blanchet L, Lebrec D. Measurement of hepatic blood flow and diethyl-ida in man: Comparison with indocyanine green. *Eur J Nucl Med* 1982; **7:** 526–527.
26. Ohnhaus EE, Noelpp UB, Ramos R *et al*. A modification of the Xe-133 inhalation method for the measurement of liver blood flow in man. *Eur J Nucl Med* 1985; **10:** 125–128.
27. Ha-Kawa SK, Tanaka Y. A quantitative model of technetium-99m-DTPA-galactosyl-HAS for the assessment of hepatic blood flow and hepatic binding receptor. *J Nucl Med* 1991; **32:** 2233–2240.
28. Cohn JN, Khatri IM, Groszmann RJ *et al*. Ratio of hepatic blood flow in alcoholic liver measured by an indicator dilution technique. *Am J Med* 1972; **53:** 704–714.
29. Mathie RT. Hepatic blood flow measurement with inert gas clearance. *J Surg Res* 1986; **41:** 92–110.
30. Yasihara Y, Miyauchi S, Hammamoto K *et al*. Measurement of regional portal blood flow with Xe-133 and balloon catheter in man. *Eur J Nucl Med* 1989; **15:** 346–350.